A Cramer-Rao Bound on Acoustic Measurement of Ocean Climate Change in the Presence of Mesoscale Sound-Speed Variability

Jeffrey L. Krolik and Sunil Narasimhan
Department of Electrical Engineering, Duke University
Durham, N.C., 27708-0291

Abstract

The ability to measure climate-related mean changes in ocean temperature is fundamentally limited by the presence of mesoscale variability. In this paper, the Cramer-Rao Lower Bound on the estimation of the mean depth-dependent temperature profile is evaluated to determine the highest accuracy which could be achieved by acoustic thermometry of ocean climate (ATOC). Evaluation of the bound is performed using a model of sound-speed variability derived from real Pacific ocean environmental data. Results indicate that a low-order Chebyshev polynomial may be a good choice for climate signal representation. The general behavior the bound is determined by a subtle interaction between the climate signal basis, *a priori* mesoscale noise statistics, and observation-time-bandwidth-signal-to-noise ratio product.

I. Introduction

The measurement of ocean temperature changes over large spatial-scales (>500 km.) provides both a means of monitoring global warming as well as the data necessary to validate coupled ocean-atmosphere climate models. However the estimation of large spatial-scale changes in ocean temperature is fundamentally limited by the presence of mesoscale (~100 km.) temperature variability. Because ocean acoustic propagation depends on the range-averaged sound-speed (and hence temperature) profile, long-range acoustic transmissions have been proposed as a means of filtering out mesoscale variability in order to measure a global warming related trend in the large spatial-scale temperature distribution [1], [2].

In this paper, the Cramer-Rao Lower Bound (CRLB) on the estimation of the mean depth-dependent temperature profile in the presence of mesoscale sound-speed variability is evaluated to determine the fundamental accuracy limits which could be achieved by ATOC. This paper extends previous work where a CRLB has been derived assuming a fully-spanning array and limited signal bandwidth such that the modal group delays are sufficient statistics for the global warming signal [3]. In this paper, a more general bound applicable to non-fully-spanning broadband arrays is discussed.

II. Stochastic Environmental and Acoustic Propagation Modeling of the Ocean Environment

Consider an underwater acoustic waveguide with a random range-dependent sound-speed profile, $c(z, r)$, given by:

$$c(z, r) = c_o(z) + \Delta c(z, r) \tag{1}$$

where $c_o(z)$ is the assumed background sound-speed profile and $\Delta c(z, r) \ll c_o(z)$ is a random sound-speed perturbation. The sound-speed perturbation $\Delta c(z, r)$ consists of an unknown nonrandom mean "climate-signal" component, $\delta c(z)$ plus a random mesoscale component represented in terms of empirical orthogonal functions (EOF's), $\psi_l(z)$, [5] so that:

$$\Delta c(z, r) = \delta c(z) + \sum_{l=1}^{L} g_l(r)\,\psi_l(z) \tag{2}$$

where the $g_l(r), l = 1, \ldots, L$ are zero-mean stationary random processes with variances $\sigma^2_{g_l}$ that describe the range dependence of each mesoscale component. To estimate the mean sound-speed profile or equivalently $\delta c(z)$ express:

$$\delta c(z) = \sum_{m=0}^{M-1} b_m T_m(z) \tag{3}$$

where the functions $T_m(z)$ define a basis for the space of climate signals which can be estimated without bias.

Acoustic thermometry consists of long range transmission of a known T second broadband acoustic source signal to a vertical receiving array of M_s sensors. In an adiabatic acoustic ocean waveguide supporting N normal modes, applying first-order perturbation theory, the vector of Fourier coefficients of the array outputs at frequency $\omega_k = 2\pi k/T$ due to a source at range r_s and depth z_s in the presence of Gaussian zero-mean additive noise $\boldsymbol{n}(\omega_k)$ can be expressed as [4]:

$$\boldsymbol{x}(\omega_k) = \frac{a(\omega_k)}{\sqrt{r_s}} U_o S_o \boldsymbol{v} + \boldsymbol{n}(\omega_k) \tag{4}$$

where the mn^{th} element of the $M_s x N$ matrix U_o is $\varphi_n^{(o)}(z_m)$, the n^{th} diagonal element of the NxN diagonal matrix S_o is $\sqrt{2\pi}\left(\varphi_n^{(o)}(z_s)/\sqrt{k_n^{(o)}}\right)e^{jk_n^{(o)}r_s}$, and the vector

0-7803-2431-5/95 $4.00

$v(\boldsymbol{b}, \bar{\boldsymbol{g}}) = exp(j\Delta_b \boldsymbol{b} + j\Delta_g \bar{\boldsymbol{g}})$. The $\varphi_n^{(o)}(z)$ and $k_n^{(o)}$ are respectively modal depth eigenfunctions and horizontal wavenumbers corresponding to the waveguide with background profile $c_o(z)$. The l^{th} element of the *Lx1* vector $\bar{\boldsymbol{g}}$ is given by $\bar{g}_l(r_s) = \int_0^{r_s} g_l(r)\,dr$ and *exp(x)* denotes the element-wise exponential function. The nl^{th} element of the *NxL* matrix Δ_g is given by:

$$\{\Delta_g\}_{nl} = \frac{-1}{k_n^{(o)}} \int_0^{\infty} \frac{\left|\varphi_n^{(o)}(z)\right|^2 \left(k^{(o)}(z)\right)^2}{c_o(z)} \psi_l(z)\,dz \qquad (5)$$

i.e. the n^{th} horizontal wavenumber perturbation due to the l^{th} mesoscale EOF. The nl^{th} element of Δ_b is defined by Eq. (5) but with $r_s T_l(z)$ associated with the l^{th} climate signal basis function replacing $\psi_l(z)$

Given a source of bandwidth W Hertz and $T \gg$ noise correlation time, acoustic thermometry consists of estimating $\boldsymbol{b} = [b_o, \ldots, b_{M-1}]^T$ in the presence of the random mesoscale parameter vector, $\bar{\boldsymbol{g}}$, using the TW uncorrelated frequency-domain snapshots, $\boldsymbol{x}(\omega_l), \ldots, \boldsymbol{x}(\omega_h)$, over the signal frequency band from ω_l to ω_h . Substituting the estimated $\hat{\boldsymbol{b}}$ into Eq. (3), the estimated temperature perturbation, $\delta T(z)$, is obtained from $\delta T(z) \approx \delta c(z) \frac{\partial T}{\partial c}$ where $\frac{\partial T}{\partial c}$ can be computed from the Del Grosso equation relating sound-speed and temperature [6].

III. A Hybrid CRLB for Acoustic Measurement of the Climate Change Signal

In light of the climate signal representation of Eq. (3), the CRLB on estimates of $\delta c(z)$ can be expressed as:

$$Var(\delta c(z)) \geq \boldsymbol{T}(z)^T \boldsymbol{J}^{-1}(\boldsymbol{b})\,\boldsymbol{T}(z) \qquad (6)$$

where $\boldsymbol{J}(\boldsymbol{b})$ is the Fisher Information Matrix (FIM) for $\boldsymbol{b}$ and $\boldsymbol{T}(z) = [T_0(z), \ldots, T_{M-1}(z)]^T$. In the present case, the unknown parameter vector is defined by $\theta = \left[\boldsymbol{b}^T, \bar{\boldsymbol{g}}^T\right]^T$ which includes both unknown deterministic and random parameters. Because of the difficulty in computing $\boldsymbol{J}(\boldsymbol{b})$ in such "mixed" cases, a "hybrid" CRLB derived by Rockah [7] is applied here:

$$Cov(\hat{\theta}(\boldsymbol{x})) \geq \left(E_{\bar{\boldsymbol{g}}}(\boldsymbol{J}(\theta)) + \boldsymbol{J}_2\right)^{-1} \qquad (7)$$

where $\{\boldsymbol{J}_2\}_{ij} = E_{\bar{\boldsymbol{g}}}\left\{\frac{\partial^2}{\partial \bar{g}_{i-M} \partial \bar{g}_{j-M}} \ln f(\bar{\boldsymbol{g}})\right\}$ for indices i or $j = M, \ldots M+L$ and zero otherwise. Note that $f(\bar{\boldsymbol{g}})$ is the *a priori* probability density of the mesoscale parameters. Since the source range is large relative to the correlation range of the mesoscale perturbations, the Central Limit Theorem implies that $f(\bar{\boldsymbol{g}})$ is approximately Gaussian quite independent of the distribution assumed for $g_l(r)$.

The complete derivation of the hybrid CRLB of Eq. (7) for the acoustic and environmental model described in section 2 is given in [8]. Here the behavior of the bound is illustrated by considering some limiting cases where $E_{\bar{\boldsymbol{g}}}(\boldsymbol{J}(\theta))$ can be simplified. In particular, consider the case where the signal bandwidth, W, is small, the noise is spatially uncorrelated and the array is fully-spanning. In this case, the hybrid bound is given by:

$$Var(\delta c(z)) \geq \boldsymbol{T}(z)^T \boldsymbol{J}_h^{-1} \boldsymbol{T}(z) \equiv B_h(z) \qquad (8)$$

The FIM $\boldsymbol{J}_h$ can be expressed as:

$$\boldsymbol{J}_h = \boldsymbol{K}_b^H \boldsymbol{K}_b - \boldsymbol{K}_b^H \left[\boldsymbol{K}_g \left(\boldsymbol{K}_g^H \boldsymbol{K}_g + \boldsymbol{R}_{\bar{\boldsymbol{g}}}^{-1}\right)^{-1} \boldsymbol{K}_g^H\right] \boldsymbol{K}_b \qquad (9)$$

where $\boldsymbol{K}_b = \sqrt{2TW\xi \boldsymbol{A}_s}\,\Delta_b$, $\boldsymbol{K}_g = \sqrt{2TW\xi \boldsymbol{A}_s}\,\Delta_g$ and $\sqrt{\boldsymbol{A}_s}\sqrt{\boldsymbol{A}_s} = diag\left(2\pi\left(\left|\varphi_n^{(o)}(z_s)\right|^2 / k_n^{(o)}\right)\right)$. The signal-to-noise ratio (SNR) at the receiving array is denoted by ξ . The *LxL* correlation matrix of $\bar{\boldsymbol{g}}$ is $\boldsymbol{R}_{\bar{\boldsymbol{g}}} = diag\left(\sigma_{\bar{g}_l}^2\right)$ where $\sigma_{\bar{g}_l}^2$ is the variance of $\bar{g}_l(r_s)$. For a simple lowpass mesoscale horizontal process with correlation length, r_l then $\sigma_{\bar{g}_l}^2 \equiv \sigma_{g_l}^2 r_l r_s$. From Eq. (9) at a sufficiently high SNR such that $\boldsymbol{K}_g^H \boldsymbol{K}_g \gg \boldsymbol{R}_{\bar{\boldsymbol{g}}}^{-1}$, $\boldsymbol{J}_h$ can be expressed as:

$$\boldsymbol{J}_h = \boldsymbol{J}_n + \boldsymbol{R}_g^{-1} \boldsymbol{K}_b^H \left[\boldsymbol{K}_g \left(\boldsymbol{K}_g^H \boldsymbol{K}_g\right)^{-2} \boldsymbol{K}_g^H\right] \boldsymbol{K}_b \qquad (10)$$

where $\boldsymbol{J}_n$ is the FIM for the estimation of the mean sound-speed parameters in the presence of *nonrandom* unknown $\bar{\boldsymbol{g}}$. The second term on the right-hand side of Eq. (10) corresponds to the increase in information due to knowledge of the prior distribution on $\bar{\boldsymbol{g}}$. The least informative scenario corresponds to the case when the mesoscale EOF's are also the climate signal basis functions. In this

case. $J_n = 0$ and Eq. (10) becomes simply $J_h = diag\{r_s/r_l\sigma_l^2\}$. This performance corresponds intuitively to what could be achieved by simply averaging the random mesoscale process over the source range r_s.

Another case of interest is when the signal bandwidth is small and the noise is spatially uncorrelated, but the sensor array does *not* fully span the water column. In this situation, for large $\sigma_{g_l}^2$, and assuming $\Delta_{g,ml} - \Delta_{g,nl} \neq 0$ for all $m \neq n$ the mesoscale variability essentially decorrelates the modes and now:

$$J_h = 2TW\xi\left[\Delta_b^H A_u \Delta_b\right] - (2TW\xi)^2 \times \Delta_b^H A_u \Delta_g \left(2TW\xi \Delta_g^H A_u \Delta_g + R_g^{-1}\right)^{-1} \Delta_g^H A_u \Delta_b \quad (11)$$

where the elements of the diagonal matrix $\{A_u\}_{nn} = diag\left(2\pi\left|\varphi_n^{(o)}(z_s)\right|^2 \sum_{m=1}^{M_s}\left|\varphi_n^{(o)}(z_m)\right|^2 / k_n^{(o)}\right)$. Note that Eq. is comparable to the fully-spanning array case with the diagonal elements of A_s weighted by the norm of each modal eigenfunction sampled at the array elements. Further, observe that in the case of a single sensor receiver, the bound is unchanged when source depth and receiver depth are interchanged as might be expected due to the reciprocal nature of acoustic propagation under this model.

IV. Evaluation of the CRLB in Pacific Environment

In this section, the CRLB for measurement of the mean temperature profile is numerically evaluated for a Pacific deep-water ocean environment using a realistic representation of mesoscale sound-speed variability. The acoustic source is assumed to have a flat bandpass energy spectrum from 50 to 70 Hz. The numerical normal mode propagation model KRAKEN [9] was used to compute the required depth eigenfunctions and horizontal wavenumbers of the channel across the signal frequency band. The Pacific environmental data was obtained using first and second-order sound-speed profile statistics derived from a set of approximately 200 CTD, AXBT, XBT, and XSV measurements over a range of approximately 1000 km. in the North-East Pacific in July, 1989 [10]. The background profile and first five mesoscale basis functions normalized by the associated mesoscale component standard-deviation, i.e. $\sigma_{g_l}\psi_l(z), l = 1, \ldots, 5$ for this data set are shown in Figure 1. The first five EOF's accounted for over 95% of the variation in the mesoscale dataset. Since there was insufficient data to estimate range correlation distances, $r_l = 100$ km. corresponding roughly to the scale of mesoscale inhomogeneities was assumed for each component.

To represent a general class of climate signals, a finite-order Chebyshev polynomial basis was used. In order to summarize estimator performance at all depths, $B_h^u = \sqrt{\max_z\{B_h(z)\}}$, was calculated where the maximum is taken over $z = 0$ to $z = 2000$ which includes all depths where climate-related changes are expected to occur. Note that B_h^u is a lower bound on the maximum mean temperature estimate standard deviation over depth.

Figure 1 Background Profile and Mesoscale Basis Set

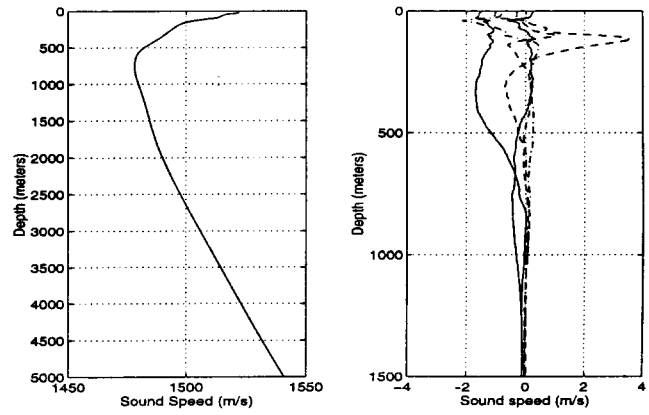

The behavior of the CRLB on mean temperature estimation as a function of observation-time-SNR product at a fully-spanning receiving array is shown in Figure 2 and Figure 3. The true climate signal is assumed to be a decaying exponential with a maximum at the ocean surface. The source is assumed to be at the sound-speed channel-axis depth of 700 m. and range of 5000 km. Two climate signal basis sets are considered: 1) Figure 2 corresponds to the case where the exponential climate signal shape is assumed known, and 2) Figure 3 corresponds to the case where a sixth-order Chebyshev polynomial basis set is used. The curves labeled "Known mesoscale" correspond to the CRLB when the random mesoscale component is assumed known and equal to zero. The curves labeled "Random mesoscale" correspond to the CRLB when the random mesoscale component is present. Note that in both figures, three regions can be identified: 1) low $T\xi$, where the "known" and "random" mesoscale curves are equal indicating that estimation performance is additive noise limited, 2) intermediate $T\xi$ where the "random" mesoscale curve is relatively flat and the bound is limited by the *a priori* mesoscale component variances, $\sigma_{g_l}^2$, and 3) high $T\xi$ where the bound is limited by the difficulty in jointly estimating $\boldsymbol{b}$ and $\bar{\boldsymbol{g}}$. The threshold values of $T\xi$ which define these regions are a non-trivial function of the climate signal basis and mesoscale statistics. For the known climate signal shape case, Figure 2 indicates that the presence of mesoscale variability dramatically increases the bound. For the Chebyshev signal case, Figure 3 indicates that the mesoscale variability has less affect on the bound. Comparing the "random" mesoscale curves of Figure 2 and Figure 3 indicates that in the presence of random mesoscale noise, only a slight increase in the bound over the signal known case occurs when a Chebyshev signal basis is used. Therefore a low-order Chebyshev polynomial basis set appears to be good choice of climate signal representation for ATOC.

Figure 2 CRLB Using Exponential Signal Basis

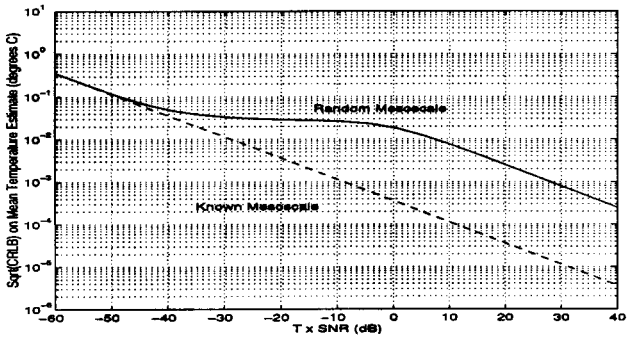

Figure 3 CRLB Using Chebyshev Signal Basis

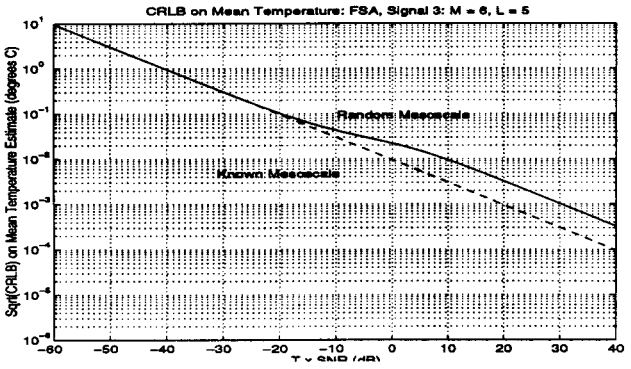

The final figure illustrates the effect on climate signal estimation performance of decreasing the receiving array length. The bounds in Figure 4 are for the Chebyshev climate signal and $T\xi$ = 30 dB. The sensor array is assumed to be centered at the sound channel axis with an inter-element spaced of 8 m. Observe that both the hybrid CRLB and the known-mesoscale CRLB decrease as the number of sensors increases. The bounds as a function of number of sensors are plotted out to 175 elements equivalent to an array length of 1400 m. which corresponds to the SOFAR channel depth. Note that at the array length maximum, the bounds agree with the fully-spanning results in Figure 3. For shorter arrays of less than ten sensors, as proposed in the GAMOT experiments [2] observe that the bounds are considerably higher.

Figure 4 CRLB versus Receiving Array Length

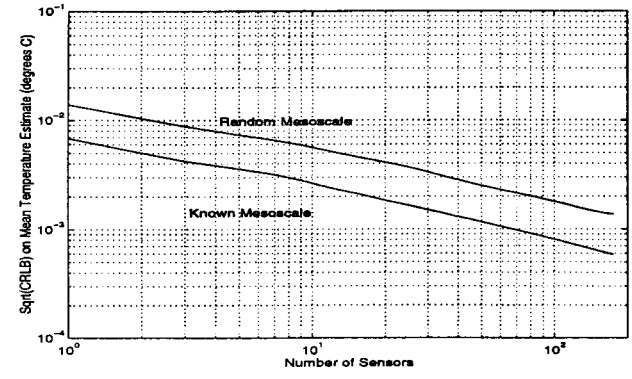

V. Conclusion

It should be noted that the bounds evaluated here assume only a single acoustic transmission is available and thus do not account for the performance gain which could be achieved by averaging mean profile estimates over multiple time periods corresponding to different mesoscale sound-speed profile realizations. Finally, a limitation of the CRLB presented here is that it assumes strictly adiabatic long range propagation. In recent work [11], it has been suggested that small-scale internal wave fluctuations cause non-adiabatic acoustic scattering which can be seen over long ranges. Taking this phenomena into account would likely result in somewhat higher bounds on acoustic thermometry of ocean climate.

Acknowledgments

The authors would like to thank Prof. Arthur Baggeroer of MIT for making available his unpublished results on this problem. This work was supported by ONR grant no. N00014-93-1-0748.

References

1 Munk, W.H.; Spindel, R.C.; Baggeroer, A.; Birdsall, T.G. "The Heard Island feasibility test". *J. Acoust. Soc. Am.*, vol. 96, no. 4, pp. 2330-42, 1994.

2 Spiesberger, J.L.; Frye, D.E.; O'Brien, J.; Hurlburt, H. et.al. "Global Acoustic Mapping of Ocean Temperatures (GAMOT)", *Proceedings of OCEANS '93,* Victoria, BC, Canada, vol. 1, pp. I253-7, 1993.

3 Baggeroer, A.B. "Modal group delay variability and the estimation accuracy of vertical arrays for monitoring ocean warming trends", unpublished manuscript, 1994.

4 Narasimhan, S., Krolik, J.L., "Fundamental limits on acoustic source range estimation performance in uncertain ocean channels", to appear *J. Acoust. Soc. Am.*, vol. 97, no. 1, 1995.

5 LeBlanc, L.R. and Middleton, F.H., "An underwater acoustic sound velocity data model", *J. Acoust. Soc. Am.*, vol. 67, pp. 2055-2062, 1980.

6 Del Grosso, V.A., "New equations for the speed of sound in natural waters" *J. Acoust. Soc. Am.*, vol. 56, no. 4, pp. 1084-91, 1974.

7 Rockah, Y. *Array Processing in the Presence of Uncertainty,* Ph.D. thesis, Yale University, 1986.

8 Krolik, J.L. and Narasimhan, S., "Performance bounds on acoustic thermometry of ocean climate in the presence of mesoscale sound-speed variability", submitted to *J. Acoust. Soc. Am.*, 1994.

9 Porter, M.B., and Reiss, E.L., "A numerical method for bottom interacting ocean acoustic normal modes", *J. Acoust. Soc. Am.*, vol. 77, pp. 1760-1767, 1985.

10 Boyd, J.D., Linzell, R.W., "Environmental data inventory VAST-I, July 1989", NOARL Technical Note no. 13, NOARL, January 1990.

11 Colosi, J.A., Flatte, S.M., Bracher, C. "Internal-wave effects on 1000-km oceanic acoustic pulse propagation: Simulation and comparison with experiment", *J. Acoust. Soc. Amer.*, vol. 96, no.1, pp. 452-468, 1994.